# Accepted Manuscript


Novel phenanthridin-6(5*H*)-one derivatives as potent and selective BET bromodomain inhibitors: Rational design, synthesis and biological evaluation

Yanle Zhi, Shu Wang, Wenhai Huang, Shenxin Zeng, Meihao Liang, Chixiao Zhang, Zhen Ma, Zunyuan Wang, Zhimin Zhang, Zhengrong Shen

PII: S0223-5234(19)30594-X

DOI: https://doi.org/10.1016/j.ejmech.2019.06.067

Reference: EJMECH 11470

To appear in: *European Journal of Medicinal Chemistry*

Received Date: 14 May 2019

Revised Date: 12 June 2019

Accepted Date: 24 June 2019

Please cite this article as: Y. Zhi, S. Wang, W. Huang, S. Zeng, M. Liang, C. Zhang, Z. Ma, Z. Wang, Z. Zhang, Z. Shen, Novel phenanthridin-6(5*H*)-one derivatives as potent and selective BET bromodomain inhibitors: Rational design, synthesis and biological evaluation, *European Journal of Medicinal Chemistry* (2019), doi: https://doi.org/10.1016/j.ejmech.2019.06.067.

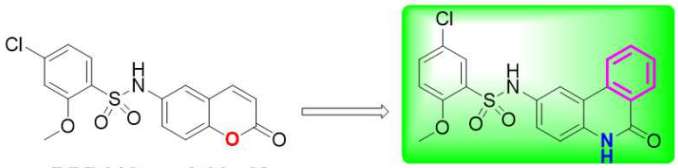


**BRD4 $IC_{50}$ = 0.93 μM**
**A549 cell line $IC_{50}$ = 4.63 μM**

**BRD4 $IC_{50}$ = 0.24 μM**
**A549 cell line $IC_{50}$ = 0.75 μM**
***invo*: $T_{1/2}$ = 3.87 h F% = 36.60%**

**24**

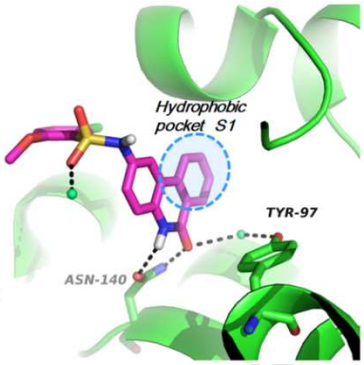

# Novel phenanthridin-6(5*H*)-one derivatives as potent and selective BET bromodomain inhibitors: rational design, synthesis and biological evaluation

Yanle Zhi[a], Shu Wang[b], Wenhai Huang[b], Shenxin Zeng[b], Meihao Liang[b], Chixiao Zhang[b], Zhen Ma[b], Zunyuan Wang[b], Zhimin Zhang[b,*],Zhengrong Shen[b,*]

[a]*College of Pharmacy, Henan University of Traditional Chinese Medicine, Zhengzhou 450046, Henan Province, P. R. China*

[b]*Key Laboratory of Neuropsychiatric Drug Research of Zhejiang Province, Institute of Materia Medica, Zhejiang Academy of Medical Sciences, Hangzhou, 310013, P. R. China*

**Correspondence**

Zhimin Zhang, Institute of Materia Medica, Zhejiang Academy of Medical Sciences, Hangzhou 310013, P. R. China Tel.: +86 571 88215626; fax: +86 571 88215625.
E-mail address: zzm996@126.com

Zhengrong Shen, Institute of Materia Medica, Zhejiang Academy of Medical Sciences, Hangzhou 310013, P. R. China Tel.: +86 571 88215506; fax: +86 571 88215625.
E-mail address: shenzr601@163.com

# Novel phenanthridin-6(5*H*)-one derivatives as potent and selective BET bromodomain inhibitors: rational design, synthesis and biological evaluation

## Abstract

Inhibition of BET family of bromodomain is an appealing intervention strategy for several cancers and inflammatory diseases. This article highlights our work toward the identification of potent, selective, and efficacious BET inhibitors using a structure-based approach focused on improving potency. Our medicinal chemistry efforts led to the identification of compound **24**, a novel phenanthridin-6(5*H*)-one derivative, as a potent ($IC_{50}$ = 0.24 μM) and selective BET inhibitor with excellent cancer cell lines inhibitory activities and favorable oral pharmacokinetic properties.

**Keywords:** Rational drug design; BET bromodomain inhibitor; antiproliferative effect; apoptosis; pharmacokinetics

## 1. Introduction

The bromodomain and extra-terminal (BET) family of proteins are epigenetic readers which mediate the expression of therapeutically important genes such as C-myc through the selective recognition of acetylated histones [1]. The BET proteins consist of bromodomain containing protein 2 (BRD2), BRD3, BRD4, and the testis-specific BRDT and have been positively recognized as promising therapeutic targets for the treatment of cancer, inflammation [2], and viral infectious diseases [3, 4]. BRD4, the most extensively studied member, has been shown to recruit the positive transcription elongation factor b (P-TEFb), and regulated the phosphorylation

of the RNA polymerase □ in the transition from transcription initiation to productive elongation [5, 6]. BRD4 contains two *N*-terminal bromodomains (BD1 and BD2) that selectively bind to acetylated lysine (KAc) in histones H3 and H4 [7]. More specifically, the KAc residues bind in the active site of BRD4 with an evolutionarily conserved asparagine (Asn140) that acts as a hydrogen bond donor, and through an interaction between the acetyl carbonyl oxygen atom and the phenol of a conserved tyrosine (Tyr97) via a structured water molecule [8]. Disrupting the protein-protein interactions between bromodomain and KAc by inhibitors can be a viable therapeutic target for many diseases [9, 10]. In the last few years, a number of high-affinity small molecule BET inhibitors have been identified [11-16]. Till now, over 20 clinical trials are underway for studying the effects of BET family inhibition as anti-cancer or anti-inflammatory therapies [17, 18]. Most reported inhibitors act as pan-BET bromodomain inhibitors due to the high sequence identity among BET proteins. JQ-1 (**1**) [19] and I-BET151 (**2**) (figure 1) [20] were first demonstrated the therapeutic potential of BET bromodomain inhibitors and have been extensively employed to evaluate the biological functions of BET bromodomain. Compounds **3**-**6** (figure 1) are currently in phase I and phase II clinical trials for treatment of solid tumors and hematological malignancies [16]. Compound **6** was initially described to upregulate ApoA1 expression and increase the high-density lipoprotein mass and has recently been reported to be a BET inhibitor [21, 22]. Considering these many phenotypes and strategies of therapeutic relevance, novel chemotypes of BET inhibitors are being intently pursued.

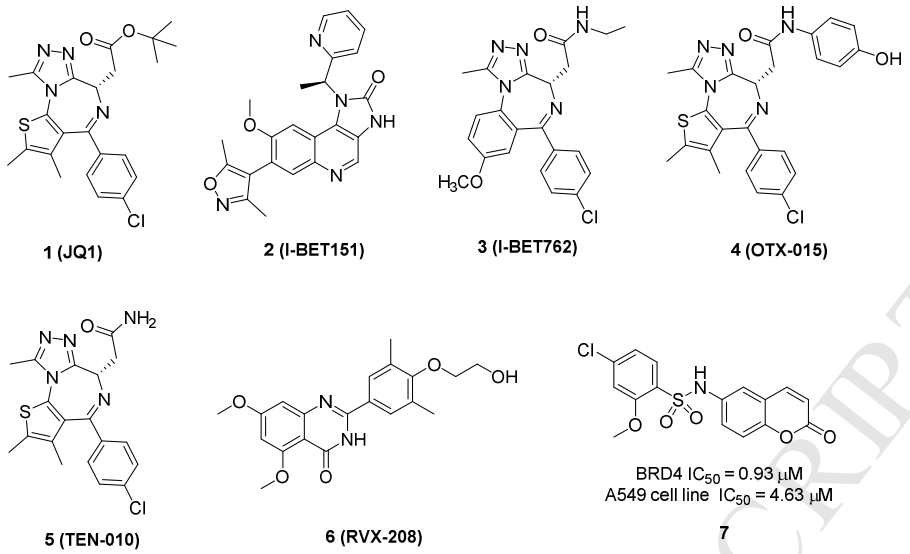


**Figure 1**. Structures of typical BET bromodomain inhibitors JQ1 (**1**), I-BET151 (**2**), I-BET762 (**3**), OTX-015 (**4**), TEN-010 (**5**), RVX-208 (**6**) and our previously reported compound **7.**

In our ongoing efforts to identify potent and novel selective BET inhibitors, we recently reported 4-chloro-2-methoxy-N-(2-oxo-2H-chromen-6-yl)benzenesulfonamide (**7**) as a potent and orally bioavailable BRD4 bromodomain inhibitor [23]. Compound **7** binds to BRD4 with nanomolar affinities and shows micromolar cell growth inhibitory activities in four cell lines. Besides, compound **7** has a good pharmacokinetic profile in rats. However, compared to some other reported inhibitors [24-27], both the BRD4 affinities and cell growth inhibitory activities of compound **7** are still remained to improve. We have therefore decided to pay our efforts toward the generation of novel, highly potent, efficacious, and orally active BET bromodomain inhibitors starting from compound **7**.

By carefully analysis of the docking information of compound **7** with BRD4, we identified an unoccupied hydrophobic region within the binding site. To the best of our knowledge, few attentions have been paid to this hydrophobic region in designing novel BET bromodomain inhibitors or improving the binding affinity of reported BET

bromodomain inhibitors. In this article, focused on this significant but previously not studied hydrophobic region, we reported the design, synthesis and biological evaluation of phenanthridin-6(5*H*)-one derivatives as a novel class of BET bromodomain inhibitors with promising therapeutic effects. The SAR investigation and the pharmacological mechanisms, pharmacokinetics and *in vitro* anti-tumor activity of selected compounds were also presented.

## 2. Results and Discussion

### 2.1 Binding Site Analysis and Design of Novel Phenanthridin-6(5*H*)-one Scaffold

Better understanding the structure of protein binding site is a cornerstone of structure-based drug design. In our efforts to further improve the potency and increase structural diversity of coumarin derivatives BET inhibitors, we examined the docking formation of compound **7** in more detail with the aim of identifying areas where additional binding interaction might be gained. As shown in figure 2A, the coumarin moiety of **7** forms two hydrogen bonds with Asn140 and Tyr97 *via* a conserved water molecule in the KAc binding site of BRD4. The 4-chloro-2-methoxybenzene group occupies the hydrophobic WPF shelf and forms hydrophobic interactions with Met149, Asp144, Asp145 and Ile146. The sulfonamide forms two additional hydrogen bonds with two water molecules. In addition to these main interactions, a large space was identified within the binding site that was not fully occupied by compound **7**. We refer to this space as the “S1 pocket” (highlighted by the red patch in figure 2A). Furthermore, we applied SiteMap in the Schrödinger software suite (Schrödinger, LLC: New York 2011) to take key steps toward efficient

structure-based drug design by gaining insights into binding sites, which can be used to suggest modifications to a ligand's structure (both shape and physical properties) [28, 29]. The active site points and surfaces generated by SiteMap for BRD4 are shown in figure 2B. These figures revealed that portions of the hydrophobic groups of compound **7** occupy the hydrophobic regions, wherein the hydrogen bond donors and acceptors of the ligand for the most part lie in or close to appropriate donor and acceptor of BRD4.

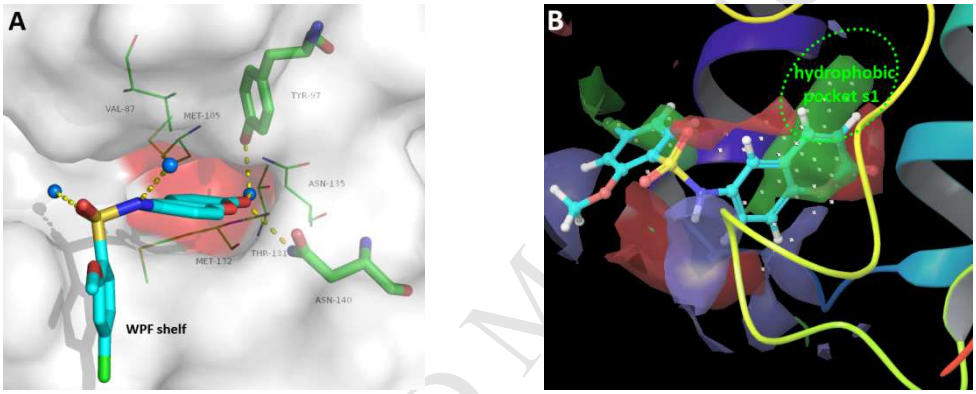


**Figure 2**. (A) The docking model of compound **7** cbound to BRD4(1) (PDB entry 3MXF). The red patch on the protein surface indicates a hydrophobic region. Compound **7** is shown in stick with carbon atoms colored in cyan, oxygen atoms in red, sulphur atoms in yellow and nitrogen atoms in blue. Water molecules are shown as blue spheres, and the hydrogen bonds were denoted by golden dash lines. The figure was prepared using PyMOL. (B) SiteMap regions for the binding of compound **7** to BRD4 displays **7** (cyan sticks) and the SiteMap site points (white spots) against the background of the protein surface. The protein backbone is shown in ribbon. The figure displays compound **7** in the context of the hydrophobic, ligand acceptor, and ligand donor maps (green, red, and purple, respectively). The figure was prepared using Schrödinger software.

The previously unexplored S1 pocket was a hydrophobic region indicated by Sitemap, which has greatly inspired our interest in this pocket. We postulated that an improvement on binding affinity might be achieved by occupying S1 pocket through

larger hydrophobic moieties. Hence, we combined a hydrophobic group (benzene ring) on the coumarin scaffold (figure 3). Moreover, replacing of the O atom of coumarin by NH might yield additional hydrogen-bond interactions for a hydrogen bond acceptor (Asn140) close to the coumarin scaffold (figure 3). To test the above hypothesis, we prepared the phenanthridin-6(5*H*)-ones derivatives and evaluated their ability to disrupt the bromodomain−KAc interaction.

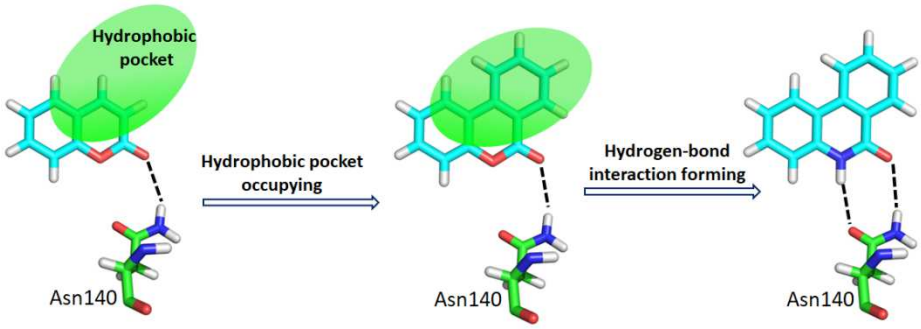


**Figure 3**. Flowchart summarizes the discovery and optimization strategy for novel phenanthridin-6(5*H*)-one scaffold from coumarin scaffold.

## 2.2 SAR Studies of the Linkers

Besides a KAc binding moiety, a typical BET inhibitor also contains a specific linker to connect a group for reaching into the hydrophobic binding site known as the WPF shelf pocket to gain essential potency and selectivity. It is believed that only the specific linkers will allow the group to extend and reach the WPF subpocket. In order to find out an optimal linker, we evaluated various sulfonamides, ureas and carbamates derivatives attached with a phenyl group. As shown in Table 1, it was found that when the linker was sulfonamide (compounds **11** and **12**) it showed better potency than those having linkers of ureas (compound **10**) or carbamates (compounds **8** and **9**). Moreover, addition of a carbon atom between the phenyl ring and sulfonyl reduced the binding activity by almost 3-folds (in comparision of compound **11** with

compound **12**).

Table 1. Results of compounds **8**-**12** on BRD4 binding activities

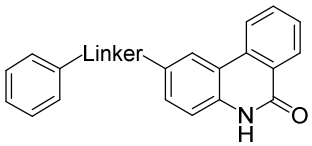


| Comp. No. | Linker | BRD4 $IC_{50}$ (μM)[a] |
|---|---|---|
| **8** | 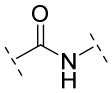 | 18.61±6.52 |
| **9** | 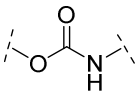 | 6.02±1.61 |
| **10** | 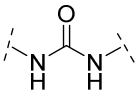 | 9.93±3.07 |
| **11** | 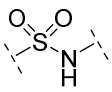 | 1.64±1.64 |
| **12** | 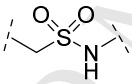 | 5.17±1.20 |

[a]The $IC_{50}$ in the table was calculated from two independent experimental measurements and expressed as mean ± SD

To better understand the remarkable difference between these linkers, we docked all the five compounds **8**-**12** to BRD4. As depicted in figure 4, only the sulfonamide group (compound **11**, carbon atoms colored in cyan) makes a turn to enable the phenyl ring go into the WPF shelf.

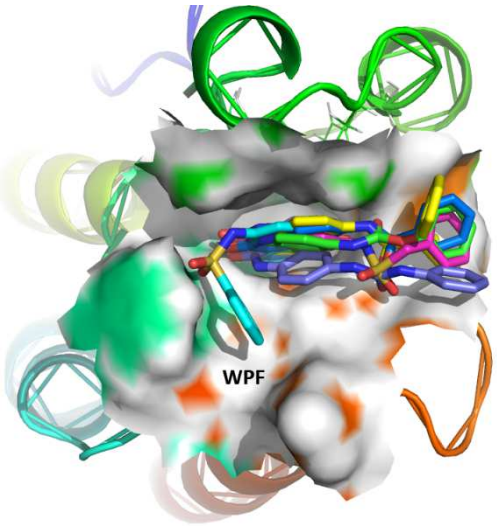


**Figure 4.** The docking model of compounds **8-13** bound to BRD4(1) (PDB entry 3MXF). **8** is shown in stick with carbon atoms colored in yellow, **9** in green, **10** in blue, **11** in cyan and **12** in pink. The figure was prepared using PyMOL.

### 2.3 SAR Studies of Sulfonamide Derivatives Occupying the WPF Shelf

Taking advantage of the above knowledge, we next explored the SAR around the WPF shelf while maintaining the sulfonamide as the linker (table 2). First, lipophilic alkyl or cycloalkyl substituted compounds **13-16** were synthesized. However, no matter the change of alky chain length or cycloalkane size, the BRD4 binding activities of **13-16** reduced markedly compared with the phenyl group substituted compound **11**. This results probably due to a reduction of hydrophobic interactions with WPF shelf. Subsequently, we focused our optimization back to the phenyl group of compound **11** which preferably occupied the hydrophobic WPF shelf. An extensive SAR exploration was then conducted, displaying that diverse substitutions at different positions of the phenyl group in compound **11** can lead to various effects on the BRD4 affinity. We preferentially evaluated the 2-chlorophenyl group and 2-methoxyphenyl group. The biochemical activity results showed that

*ortho*-substituents on the ring were very favorable. Chloro-substituent at *ortho*-position was well tolerable and the corresponding compound **17** showed comparable activity to compound **11**, while compound **18**, which bears an *ortho*-position methoxy group, showed more potent with a 3-fold increase of activity. We next investigated the *para*-position substituents (**19**-**21**). The *para*-chlorine substituted analogue **20** was somewhat more potent than *para*-tertiary butyl substituted analogue **19** and *para*-methoxyl substituted analogue **21**, which may indicate that electron-withdrawing groups at the *para*-position was favorable. We further investigated the impact of meta-position substituents (compounds **22** and **23**). Interestingly, compound **22**, which bears a meta-position cyan group showed moderate activity, while, compound **23** bears a *meta*-position chlorine resulted in a 2-fold increase of activity compared with compound **11**. From the above SAR, it was identified that chlorine at *para*-position (compound **23**) or methoxy group substituent at *ortho*-position (compound **18**) possesses the favorable affinity on BRD4, so we attempted to merge these two positions as bi-substituent. In line with our expectations, the resulting 5-chloro-2-methoxy di-substituent compound **24** significantly improved the activity with an $IC_{50}$ of 0.24 μM, almost 7-fold increase compared with compound **11.** For more understanding the SAR, we further replaced the phenyl ring of compound **11** by a smaller size thienyl group, the resulting derivative **25** showed low binding activity. The replacement by larger aromatic group also led to a reduction of affinity (compounds **26** and **27**).

**Table 2.** Results of compounds **13** -**27** on BRD4 binding activities

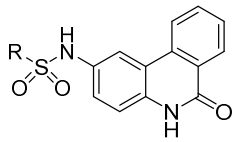

| Comp. No. | R | BRD4 $IC_{50}$ (μM)[a] | cLogP[b] | LE[c] |
|---|---|---|---|---|
| **13** |  | 6.71±2.66 | 2.33 | 0.30 |
| **14** | 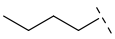 | 5.54±3.58 | 2.85 | 0.31 |
| **15** |  | 6.17+2.06 | 2.74 | 0.29 |
| **16** |  | 5.92±6.02 | 3.30 | 0.28 |
| **17** |  | 1.25±0.25 | 3.44 | 0.32 |
| **18** | 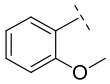 | 0.48±0.13 | 2.57 | 0.33 |
| **19** | 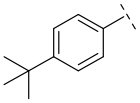 | 1.13±0.56 | 4.72 | 0.29 |
| **20** | 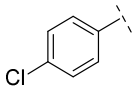 | 0.85±0.22 | 3.74 | 0.33 |
| **21** | 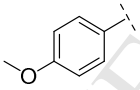 | 1.32±0.39 | 3.05 | 0.30 |
| **22** | 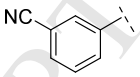 | 1.79±0.61 | 2.86 | 0.30 |
| **22** | 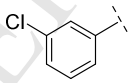 | 0.79±0.26 | 3.74 | 0.33 |
| **24** | 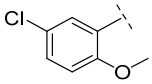 | 0.24±0.27 | 3.39 | 0.34 |
| **25** |  | 6.74±1.81 | 2.67 | 0.30 |
| **26** | 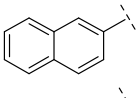 | 7.23±2.44 | 4.07 | 0.25 |
| **27** | 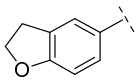 | 13.12±3.69 | 3.19 | 0.24 |
| **JQ1** | - | 0.04±0.05 | 4.82 | 0.33 |

[a]The $IC_{50}$ was calculated from the AlphaScreen assay. [b]cLogP values were calculated using ChemBiodraw Ultra14.0. [c]LE (Ligand Efficiency) = 1.4 ($pIC_{50}$/heavy atoms)

### 2.4 Docking Study of the Preferred Configuration of Compound 24

To elucidate the observed activity of compound **24**, we performed a molecular docking study starting from the crystal structure of the protein complexed with **JQ1**. At first, self-docking procedure was successfully applied on **JQ1,** well reproducing the crystallographic pose of **JQ1** inside the binding site. By superimposing the cocrystal structures of **JQ1** to our docking structure of compound **24** bound to BRD4 (figure 5A), we found that these two molecule shared high overlaps. It is worth pointing out that compound **24** fits the hydrophobic region better than **JQ1**. The docking simulations (figure 5B) performed on compound **24** illustrated that the phenanthridin-6(5*H*)-one establishes two hydrogen bonds to the conserved residue Asn140 and a water-mediated hydrogen bond to Tyr97. The sulfonamide group made a right angle to introduce the 5-chloro-2-methoxybenzene moiety toward the WPF shelf. The moiety well occupied the hydrophobic WPF shelf and forms hydrophobic interactions with Met149, Asp144, Asp145, and Ile146. Moreover, the sulfonamide group itself forms two additional hydrogen bonds with two water molecules.

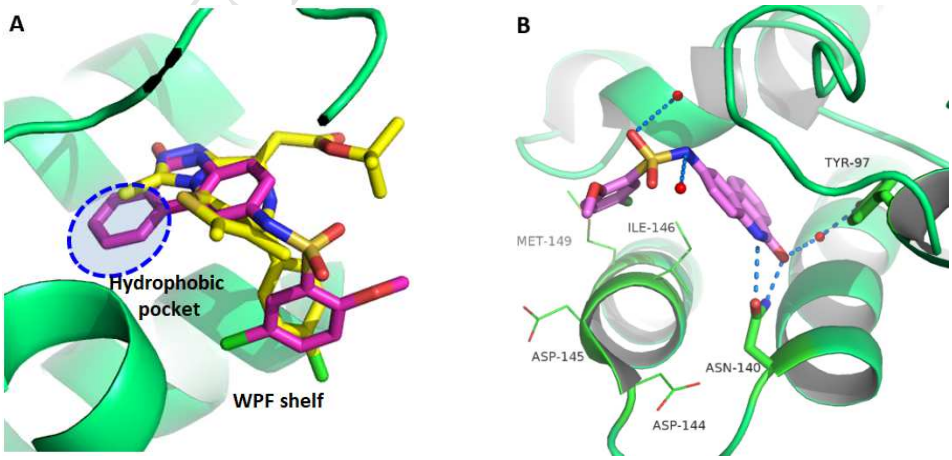


**Figure 5.** (A) Superimposed the cocrystal structure of BRD4 bound with **JQ1** and the docking model of compound **24** bound to BRD4 (PDB entry 3MXF). **JQ1** and compound **24** are shown in

stick with carbon atoms colored in yellow and magenta, respectively. (B) The docking model of compound **24** bound to BRD4 (PDB entry 3MXF). Water molecules are shown as red spheres, and the hydrogen bonds are denoted by blue dash lines. The figures were prepared using PyMOL.

### 2.5 Evaluation of the Bromodomains Selectivity of Compound 24.

It is well established that the selectivity is critical for the success of drug discovery. To investigate the selectivity profile, the compound **24** was chosen as a representative and further evaluated against a panel of BET and non-BET bromodomains. The AlphaScreen technology FRET assay was employed to test the binding tendency of compound **24**. As shown in figure 6, compound **24** showed excellent selectivity for BET bromodomains (BRD2, BRD3, BRD4 and BRDT) over other non-BET bromodomain-containing proteins. Compound **24** revealed high potency for BET family members with an affinity of > 70% under 20 μM. In addition, moderate activities for BFPF1B and BRD9 were observed, with the affinity of > 30%, which suggests that compound **24** might be a promising starting point for developing BFPF1B and BRD9 inhibitors.

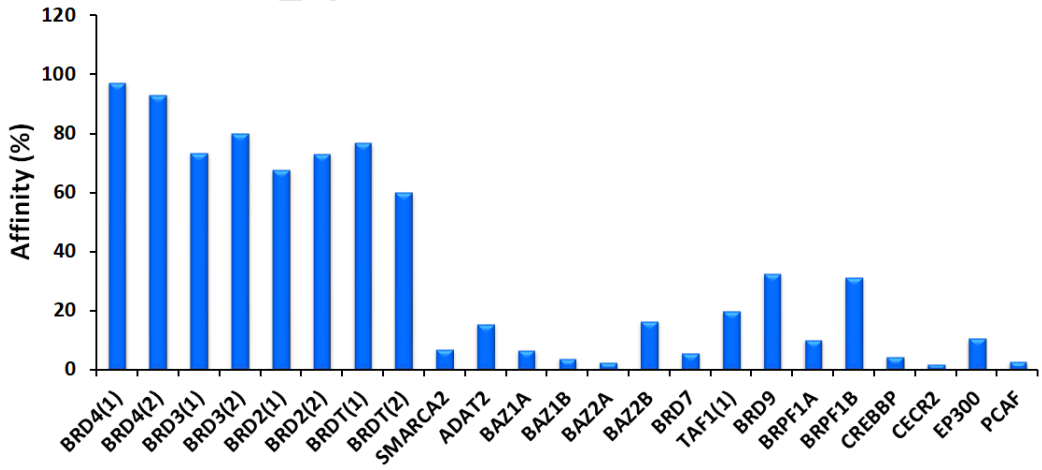


**Figure 6.** Selectivity assessments of compound **24** against BRD families. The affinity percentages were obtained at 20 μM.

### 2.6 Antiproliferative Activity of Compound 24 on Four Cell Lines

The representative compound **24** was next evaluated for its effects on the survival of four cell lines with an MTT assay. The data obtained were summarized in Table 3 and the dose–response curves were provided in figure 7. Results indicated that, consistent with its high affinity to BRD4, compound **24** potently inhibits the proliferation in these four cell lines, with $IC_{50}$ values of 0.75, 4.83, 6.70, and 5.35 μM, respectively. It is noteworthy that, in the A549 cell line, compound **24** exhibited excellent activity, which was worth in-depth study in its mechanism of anti-lung adenocarcinoma action. Overall consideration of the data from the above assays, compound **24** has good profiles for further evaluation.

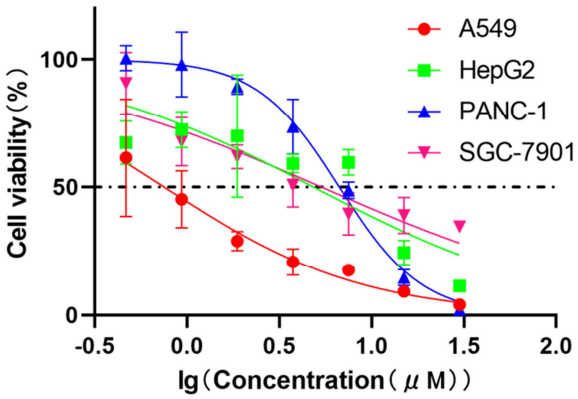


**Figure 7.** Dose–response curves of compound **24** in incubation with cancer cell lines (mean ±SD, n = 3).

Table 3. Anti-proliferation effects of compound **24** against four cell lines.

| Cancer Type | Cell Line | $IC_{50}$ (μM) |
|---|---|---|
| Lung adenocarcinoma | A549 | 0.75 |
| Hepatocellular carcinoma | HepG2 | 4.83 |
| Pancreatic carcinoma | PANC-1 | 6.70 |
| Gastric | SGC-7901 | 5.35 |

adenocarcinoma

### 2.7 Effects of Compound 24 on C-myc Protein Expression

Previous studies have shown that targeted inhibition of BET can effectively down-regulate the transcription of C-myc, an oncogene frequently overexpressed in various tumors [30, 31]. As shown in our above study, the A549 cell line is very responsive to BET inhibitors, and accordingly we examined the effect of compound **24** in A549 cells on C-myc with **JQ1** as the positive control (Figure 8). Consistent with its high binding affinities to BET proteins, the western blot data showed that compound **24** was very effective in inducing the downregulation of C-myc at a concentration as low as 100 nM in a dose dependent manner.

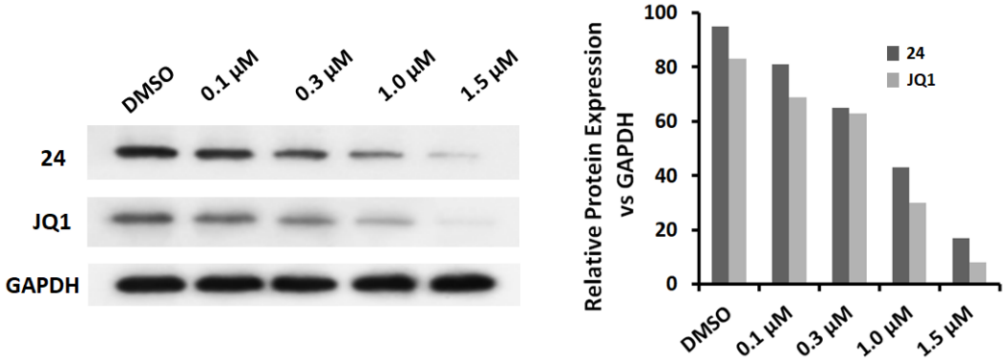


**Figure 8.** Western blotting analysis of the C-myc protein in A549 cells treated with compound **24** or **JQ1**. A549 cells were treated for 48 h at the indicated concentrations. GAPDH was used as the loading control.

### 2.8 Effect of Compound 24 on Cell Apoptosis

Inducing apoptosis is considered as one of the major strategies for antitumor-drug development. We employed flow cytometry analysis to detect the effect of compound **24** on apoptosis in A549 cells so as to further explore the anti-proliferative mechanism of compound **24**. Quantitative analysis of necrotic cells, advanced-apoptotic cells and early-apoptotic cells was investigated through an

Annexin V-FITC and PI assay. A549 cells were incubated with 0.3–5.0 μM concentrations of compound **24** for 48 h with DMSO as the negative control. As shown in Figure 9, compound **24** treatment preliminarily induced A549 cell apoptosis at a concentration as low as 0.3 μM after 48 h incubation. Compound **24** was also found to effectively induce apoptosis in a dose-dependent manner. Furthermore, compound **24** significantly induced the apoptosis of A549 with the low dose of 1.0 μM (Figure 9). The apoptosis ratios of compound **24** measured at different concentrations were 30.3% (0.3 μM), 53.9% (1.0 μM), 75.4% (3 μM), and 80.3% (5 μM).

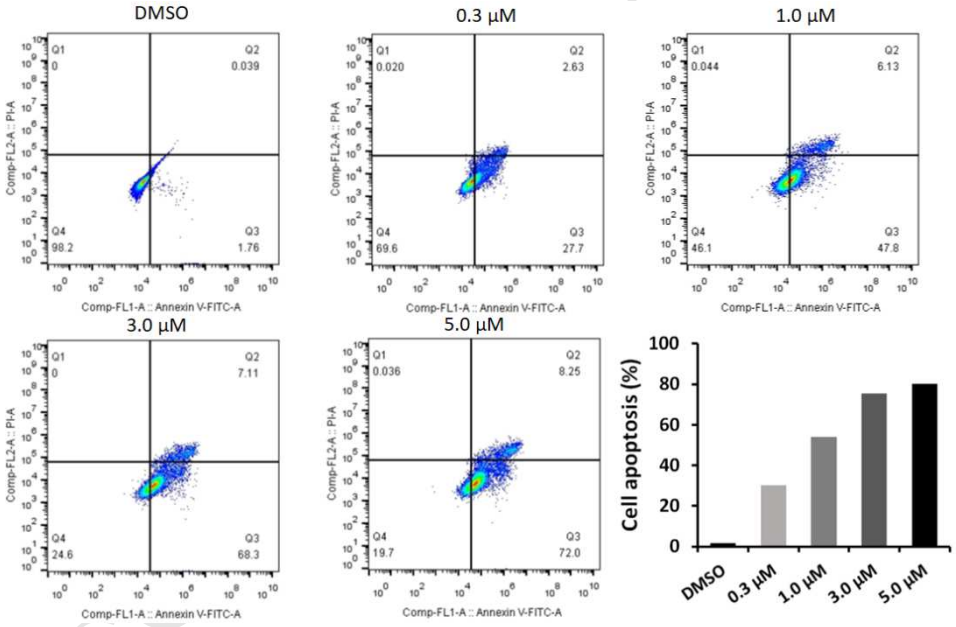


**Figure 9.** Flow cytometry analysis of apoptosis induction by compound **24** in A549 cells at the indicated concentrations for 48 h. Apoptosis was assessed by flow cytometry using Annexin V and propidium iodine (PI) double staining.

### 2.9 Effect of Compound 24 on Cell Cycle

We also employed flow cytometry analysis to investigate the ability of the compound **24** to induce cell cycle arrest in A549 cell lines. A549 cells were incubated

with 0.3–5.0 μM concentrations of compound **24** for 48 h with DMSO as the negative control. The results shown in figure 10, indicated that the cell cycle spectrum clearly changed as the compound's concentrations increased. Compound **24** arrested the cell-cycle progression of the cell line into the G1 and M phases compared with vehicle treatment in a dose-dependent manner. The percentage of cells in G1 and M phase after treatment by compound **24** under concentrations of 0.3, 1.0, 3.0 and 5.0 μM were 60.84%, 70.30%, 76.42% and 81.66%, respectively.

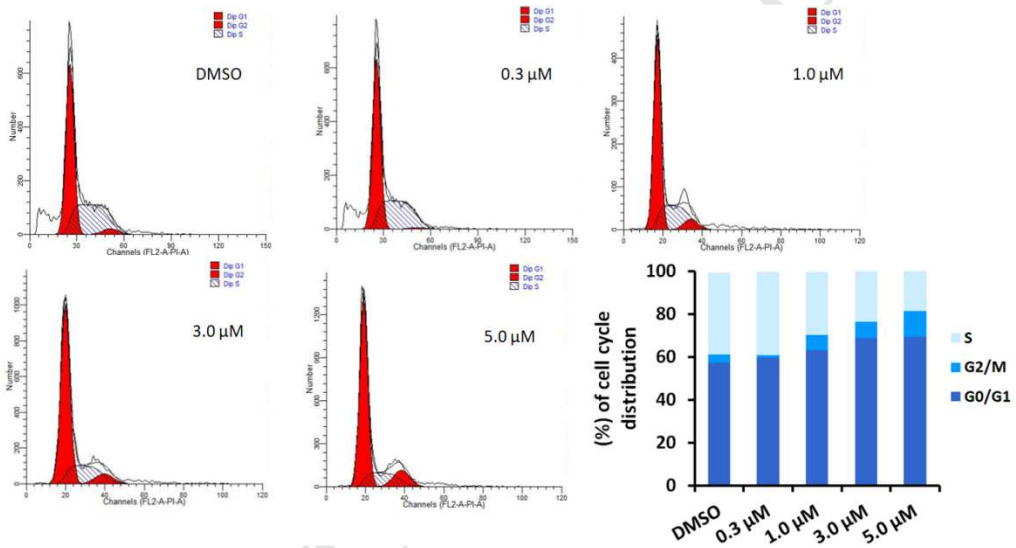


**Figure 10.** Effects of compound **24** on A549 cell cycle arrest at the indicated concentrations for 48 h.

**2.10 Microsomal Stability of** Compound **24.**

Our next attention was on assessing the selected compound **24** for its metabolic stability *in vitro* using human liver microsomes (HLMs), a system extensively employed to estimate the susceptibility to first-pass oxidative metabolism, a main cause of metabolic degradation *in vivo*. Compound **24** was incubated with HLMs at 37 °C for 2 h. The regression line of concentration-time was summarized in figure 11. The metabolic stability data indicated that compound **24** showed good microsomal

stability with half-life of 4.17 h.

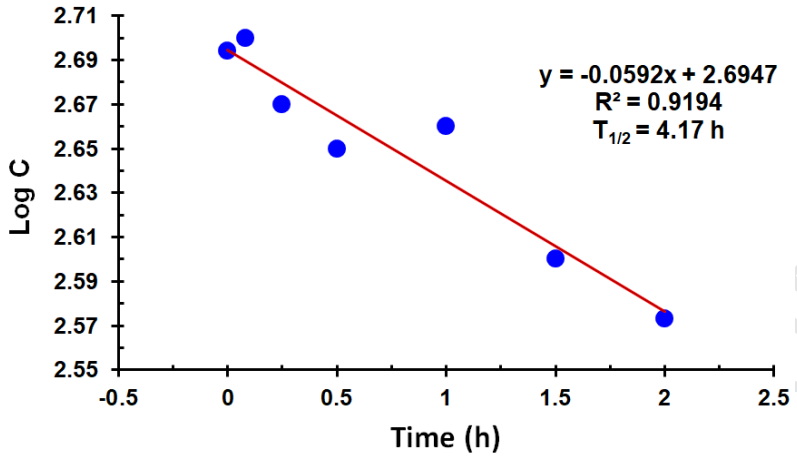


**Figure 11.** Metabolic stability of compound **24** on human liver microsomes.

### 2.11 *In vivo* Pharmacokinetic (PK) Studies of Compound 24

The favorable *in vitro* metabolic stability prompted us to evaluate compound **24** *in vivo*. Compound **24** was administered orally (p.o) or intravenously (i.v) to male Sprague-Dawley rats at a dose of 10 mg/kg and 2.5 mg/kg, respectively. The plasma concentrations were determined by liquid chromatography-tandem mass spectrometric (LC-MS/MS). The mean arterial plasma concentration-time curves were shown in Figure 12 and the pharmacokinetics parameters were concluded in Table 6. Compound **24** achieves a $C_{max}$ of 52.3 μg/L and an AUC of 565.56μg/L*h with oral administration and has an oral bioavailability (F %) of 36.6%. Compound **24** exhibited low clearance (CL) and high volume of distribution ($V_d$). Collectively, the results of this study indicated that compound **24** had favorable pharmacokinetic properties.

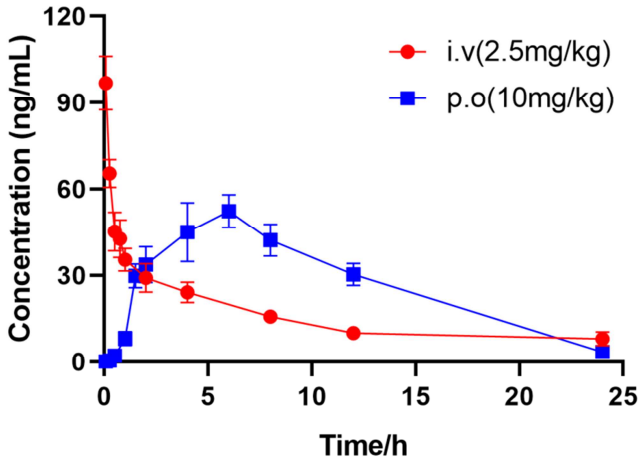


**Figure 12.** The plasma concentration-time curve of compound **24**.

**Table 4.** Intravenous (i.v.) and oral (p.o) pharmacokinetic profiles of compound **24** in rats.

| PK Parameters | i.v (2.5 mg/kg) | SD | p.o (10 mg/kg) | SD |
|---|---|---|---|---|
| $AUC_{(0-t)}$ (μg/L*h) | 383.10 | 43.54 | 565.56 | 140.89 |
| $AUC_{(0-\infty)}$ (μg/L*h) | 505.03 | 85.83 | 670.38 | 15.71 |
| $T_{1/2}$ (h) | 10.38 | 0.77 | 3.87 | 1.01 |
| $T_{max}$ (h) | 0.083 | 0 | 5.33 | 1.15 |
| $MRT_{0-t}$ (h) | 7.93 | 0.56 | 7.52 | 1.80 |
| $CL_z$ (L/h/kg) | 5.15 | 0.86 | 18.18 | 5.65 |
| $V_d$ (L/kg) | 76.70 | 10.92 | 97.34 | 8.38 |
| $C_{max}$ (μg/L) | 96.87 | 9.36 | 52.37 | 5.67 |
| F (%) | - | - | 36.60% | |

## 2.12 Chemistry

The syntheses of novel phenanthridin-6(5*H*)-one derivatives were concluded in scheme 1. As depicted, The commercially available phenanthridin-6(5*H*)-one (**I**) reacted with concentrated nitric acid in acetic acid under 100 □ to produce compound **II**. Regrettably, the reaction of compound **II** under ammonium chloride and iron powder system led to complicated mixtures, and a small quantity of the amino intermediate **III** were obtained (yield < 20%). When we tried to conduct the reduction reaction under hydrogen atmosphere, the amino intermediate **III** can be obtained with comparatively high yield (46%). The target compounds (**8-10**) were obtained by the

reactions between **III** and acyl chloride or phenyl isocyanate in $CH_2Cl_2$. The desired sulfonamide products (**11-27**) were obtained by sulphonylation reactions between **III** and various sulphonyl chlorides in pyridine, which act as solvent, as well as the base.

Scheme 1. Synthetic Route to Compounds **8-27**

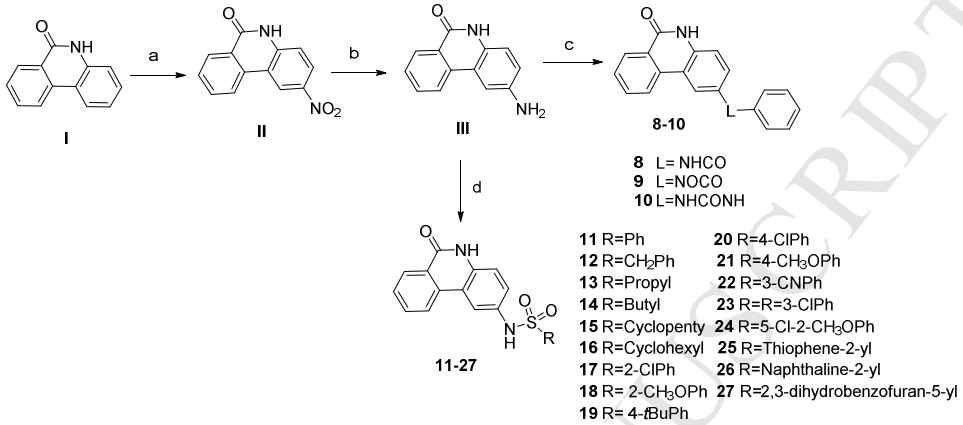


Reagents and conditions: (a) $HNO_3$/AcOH; (b) $H_2$, Pd/C; (c) $CH_2Cl_2$, $Et_3N$, acyl chloride / phenyl isocyanate (d) pyridine, sulphuryl chloride, rt.

## 3. Conclusion

In this research, a class of phenanthridin-6(5*H*)-one derivatives were designed and synthesized with the goal of obtaining novel drug-like BET Bromodomain inhibitors. Starting from our previously reported novel coumarin containing BRD4 inhibitors, a hydrophobic interaction combined with an additional key hydrogen bond interaction were identified leading to increased potency. Medicinal chemistry optimizations had led to the discovery of a set of potent and highly efficacious BET inhibitors, exemplified by compound **24**. Compound **24** bound to BET proteins with an $IC_{50}$ value of 240 nM and showed low micromolar to nanomolar potencies in four cancer cell growth inhibition. Moreover, compound **24** also significantly arrested the cell cycle distribution and induced down regulation of C-myc protein along with cell apoptosis. Testing its binding activities against other 23 bromodomain containing

proteins showed that compound **24** was also a highly selective BET inhibitor. Compound **24** demonstrated favorable human microsomal stability in vitro and acceptable oral pharmacokinetics in rats. Overall, the docking simulation study, along with the in vitro assay results demonstrated compound **24** is a promising preclinical candidate entity for the further development. More importantly, we anticipate that the phenanthridin-6(5*H*)-one scaffold, together with the newfound hydrophobic pocket, may stimulate other researchers to develop their own novel bromodomain inhibitors.

## 4. Experimental Section

### 4.1 Bromodomain Inhibition Assay

**Assay format:** The reader assay is a binding assay using AlphaScreen technology FRET assay. The biotinylated peptide binding to the reader domain of His-tagged protein is monitored by the singlet oxygen transfer from the Streptavidin-coated donor beads to the AlphaScreen Ni-chelate acceptor beads. **Reagent:** Reaction buffer: 50 mM Hepes, pH7.5, 100 mM NaCl, 0.05% CHAPS, 0.1 % BSA, and 1% DMSO (the final DMSO concentration may different depending on compound stock and test concentrations). **Bromodomain** BRD4-Full Length (**RBC Cat# RD-21-153**): Recombinant Human Bromodomain containing protein 4 (bromodomain 1 and 2; aa 2-1362; Genbank Accesstion # NM_058243), expressed in *Sf9* insect cells with an N-terminal His-tag. MW=156.5 kDa. **Ligand (C-term-Biotin)** Histone H4 peptide (1-21) K5/8/12/16Ac-Biotin**. Detection beads: PerkinElmer** Donor beads: Streptavidin-coated donor beads**.** Acceptor beads: AlphaScreen Ni acceptor beads **Reaction Procedure:** 1. Deliver 2.5X BRD in wells of reaction plate except No BRD

control wells. Add buffer instead. 2. Deliver compounds in 100% DMSO into the BRD mixture by Acoustic technology (Echo550; nanoliter range). Spin down and pre-incubation for 30 min. 3. Deliver 5× Ligand. Spin and shake. 4. Incubate for 30 min at room temperature with gentle shaking. 5. Deliver 5× donor beads. Spin and shake. 6. Deliver 5× acceptor beads. Spin and shake. Then gentle shaking in the dark for 60 min. 7. Alpha measurement (Ex/Em=680/520-620 nm) in Enspire.

**4.2 Cell Culture**

Human lung carcinoma A549 cells, Human gastric carcinoma metastatic lymph node SGC-7901 cells, human hepatocellular carcinoma HepG2 cells and human pancreatic cancer PANC-1 cells were purchased from the Cell Center of the Chinese Academy of Medical Sciences (Beijing, China). Cells were cultured in Dulbecco's modified Eagle's medium (DMEM, Gibco, Gaithersburg, MD) or RPMI 1640 medium (Gibco, Gaithersburg, MD) supplemented with 10% foetal bovine serum (FBS) and incubated at 37 □ with 5% $CO_2$ humidified atmosphere.

**4.3 Cell Growth Inhibition**

Methyl thiazolyl tetrazolium (MTT) assay was used to detect the cell survival rate. Briefly, cells were seeded into a 96-well plate at a density of $2\times10^4$ cells/mL. Medium containing a certain concentration of compound (0, 0.47, 0.94, 1.88, 3.75, 7.50, 15.0 and 30 μM) was added into each well in a volume of 100 μL for 48 h respectively. The cell morphology was observed by Invert/phase contrast microscopy (Nikon TE2000, Tokyo, Japan) (bar: 200 μm). Then 20 μL MTT solutions (Sigma, Shanghai, China) was added into each well and followed by incubation at 37°C for 4 h. 150 μL

of DMSO was further added after discarding culture medium. The crystals of formazan product were then dissolved by oscillating for 10 min. The optical density (OD) value was detected using a microplate reader (Bio-Rad, imark, USA) at a wavelength of 570 nm. The experiments were performed in triplicate. Cell survival rate (%) = (OD of administration group − OD ofblank group)/ (OD of control group − OD of blank group) × 100%. The value of inhibitory concentration 50 ($IC_{50}$) was calculated by GraphPad Prism 5 software.

**4.4 Western Blot Analysis**

To determine levels of C-myc, cells were seeded in a 6-well cell culture plate at a density of 400000 cells per well for A549 in a total volume of 1800 μL and incubated overnight in medium containing 10% fetal bovine serum (Life Technologies, Rockville, MD). Then 200 μL of serially diluted compounds were added to each well the next day. Cell lysates were harvested after 48 h and C-myc were quantified using assay kits following the manufacturer's protocols. Mouse monoclonal antibody for c-Myc was from Cell Signaling Technology (Danvers, MA, USA).

**4.5 Cell Apoptosis Assay**

The apoptosis of A549 cells was determined by Annexin V-FITC/PI assay. Annexin V binds to phosphatidylserine, which is exposed on the cell membrane and is one of the earliest indicators of cellular apoptosis. PI (Propidium Iodide) is used as a DNA stain for both flow cytometry to evaluate cell viability or DNA content in cell cycle analysis and microscopy to visualize the nucleus and other DNA containing organelles. It can be used to differentiate necrotic, apoptotic and normal cells. Cells (2

× 105) were seeded in 6-well plate and were treated with varying concentrations of inhibitor for 48 h. A549 cells were collected and incubated with FITC-conjugated Annexin V. The nuclei were then counterstained with PI. After the dual staining, the cells were screened by a FAC Scan flow cytometer (FACS Calibun, Becton Dickinson). The upper left corner of the quadrant represents debris, lower left are live cells, upper right are advanced apoptotic or necrotic cells and lower right are apoptotic cells.

**4.6 Cell Cycle Assay**

Subconfluent cells were treated with test compounds at different concentrations for 48 h. The cultures were pulse-labeled with 10 μM 5-bromo-2'-deoxyuridine (BrdU) for 30 min at 37°C prior to harvest. The cells were subsequently washed in PBS, fixed with 70% ethanol, and denatured in 2 M HCl. Following neutralization, the cells were stained with anti-BrdU fluoresceinlabeled antibodies, washed, stained with propidium iodide, and analyzed by flow cytometry using a 488 nm laser (Cell Lab Quanta SC, Beckman Coulter) 48. Cell cycle analysis was made using a FACScan cytometer (FACSCalibun, Becton Dickinson).

**4.7 Microsomal Stability Studies**

The metabolic stability was assessed using human liver microsomes (purchased from Ltd Co (RILD), M008084). Briefly, 1 μM of compound **24** was incubated with 1.7 mM cofactor β-NADPH and 0.5 mg/mL microsomes in 0.1 M phosphate buffer (pH = 7.4) containing 3.3 mM $MgCl_2$ at 37 °C. The DMSO concentration was less than 0.1 % in the final incubation system. At 0.025, 0.083, 0.25, 0.5, 1.0, 1.5 and 2 h

ofincubation, an amount of 60 μL of reaction mixture was taken out, and the reaction is stopped immediately by adding 3-fold excess of cold acetonitrile containing 100 ng/mL of internal standard for quantification. The collected fractions were centrifuged at 30 000 rpm for 5 min to collect the supernatant for LC−MS/MS analysis, from which the amount of compound remaining was determined.

**4.8 *In vivo* PK studies**

SD female rats, 6−8 weeks old， were selected for dosing. Three mice were randomly grouped per time point. Mice were received either a single intravenous injection of 2.5 mg/kg compound or a single oral administration of 10 mg/kg compound. Compounds were given as solutions in DMSO / PEG 200 / water. Blood samples were collected from rats at 0.083, 0.25, 0.5, 1, 2, 4, 6, 8, 12 and 24 h and were further processed to obtain plasma by centrifugation at 15 000 rpm for 10 min. Plasma concentrations of the compounds were determined using the liquid chromatography−tandem mass spectrometry (LC−MS/MS) method. The pharmacokinetic parameters were calculated by WinNonlin. The study was approved by the Zhejiang Academy of Medical Sciences Institutional Animal Care & Use Committee.

**4.9 Molecular Modeling**

The X-ray crystal structure of BRD4 binding with **JQ1** (PDB code: 3MXF) was retrieved from the Protein Data Bank. The protein and compounds **7** and **24** were prepared using the protein preparation wizard in Maestro with standard settings. Grids of BRD4 was generated using Glide, version 10.2, following the standard procedure

recommended by Schrodinger. The conformational ensembles were docked flexibly using Glide with standard settings in both standard and extra precision mode. Only poses with low energy conformations and good hydrogen bond geometries were considered.

### 4.10. Chemistry

#### 4.10.1. General Chemistry

Commercially available reagents and anhydrous solvents were used without further purification. The crude reaction product was purified by Flash chromatography using silica gel (300-400 mesh). All reactions were monitored by TLC, using silica gel plates with fluorescence F254 and UV light visualization. If necessary, further purification was performed on a preparative HPLC (Waters 2545) with a C18 reverse phase column. Proton nuclear magnetic resonance ($^{1}$H NMR) and carbon nuclear magnetic resonance ($^{13}$C NMR) spectra were recorded on a Bruker AV-400 spectrometer at 400 MHz. Coupling constants (*J*) are expressed in hertz (Hz). Each signal is identified by its chemical shift δ expressed in parts per million (ppm) HRMS analyzes were performed under ESI (electrospray ionization) using a TOF analyzer in V mode with a mass resolution of 9000. Melting points (mp) were determined by an M-565 melting-point apparatus with a microscope (BUCHI, made in Switzerland)

#### 4.10.2. Synthetic procedure of 2-nitrophenanthridin-6(5*H*)-one (II)

$HNO_3$ (15 ml, 65%) was added into a solution of phenanthridin-6(5*H*)-one (3.0 g, 15 mmol) in acetic acid solution (15 mL) at 0℃, the reaction mixture was stirred at room temperature for 10 min first , and then stirred at 90℃ for 4 h under nitrogen

condition. After the reaction was completed, the reaction mixture was directly filtered to obtain a filter cake, and the solid was washed with water for 3 to 4 times, and the resulting crude product was yield of 2-nitrophenanthridin-6(5H)-one (II). Without further purification, compound II was used directly to the next step according to 100% yield.

**4.10.3 Synthetic procedure of 2-aminophenanthridin-6(5*H*)-one (□)**

Palladium carbon (60 mg) and methanol solution (15 mL) were added to the flask at room temperature, and then a solution of the compound **II** in methanol was added under hydrogen atmosphere, and then the reaction solution was stirred at room temperature for about 8 h. After purification by column chromatography, compound Ⅲ was obtained in a yield of 46% (pale brown solid); mp 286.0 - 287.4 ℃. $^1$H NMR (400 MHz, DMSO-D6) δ 11.33 (s, 1H), 8.30 (d, *J* = 9.1 Hz, 1H), 8.22 (d, *J* = 8.1 Hz, 1H), 7.82 (t, *J* = 6.9 Hz, 1H), 7.59 (t, *J* = 8.0 Hz, 1H), 7.48 (d, *J* = 2.3 Hz, 1H), 7.11 (d, *J* = 8.6 Hz, 1H), 6.82 (dd, *J* = 8.6, 2.3 Hz, 1H), 5.01 (s, 2H). HRMS m/z: calcd. for $C_{13}H_{11}N_2O$ $[M+H]^+$ 211.0871, found 211.0874;

**4.10.4. General synthetic procedure of compound 8~10**

A solution of 2-aminophenanthridin-6(5*H*)-one (0.30 g, 1 mmol), corresponding sulphonyl chloride compound (1mmol) and pyridine (2 mL) in a flask was stired at room temperature for 2 h. After the reaction, ethyl acetate and a dilute hydrochloric acid solution were added for extraction, the organic layer was washed with dilute

hydrochloric acid for 3 to 4 times, and then the organic layer was concentrated to obtain the pure products.

**4.10.4.1** ***N-(6-oxo-5,6-dihydrophenanthridin-2-yl)benzamide*** **(8)** 73.2% yield (pale gray solid); mp 273.2 - 273.6 ℃. $^{1}$H NMR (400 MHz, DMSO-D6) δ 11.73 (s, 1H), 10.46 (s, 1H), 8.82 (s, 1H), 8.39 – 8.27 (m, 2H), 8.05 (d, *J* = 6.9 Hz, 2H), 7.91 (dd, *J* = 7.0, 4.0 Hz, 2H), 7.68 (t, *J* = 7.5 Hz, 1H), 7.61 (d, *J* = 8.5 Hz, 1H), 7.56 (t, *J* = 8.0 Hz, 2H), 7.39 (d, *J* = 8.8 Hz, 1H).$^{13}$C NMR (101 MHz, DMSO-D6) δ 165.9, 161.0, 135.3, 134.5, 133.4, 132.03, 128.9, 128.5, 128.1, 126.3, 123.6, 122.7, 117.9, 116.7, 115.0. HRMS m/z: calcd. for $C_{20}H_{15}N_2O_2$ $[M+H]^+$ 315.1134, found 315.1133

**4.10.4.2** ***phenyl (6-oxo-5,6-dihydrophenanthridin-2-yl)carbamate*** **(9)** 76.1% yield (white solid); mp 302.4 - 303.1 ℃. $^{1}$H NMR (400 MHz, DMSO-D6) δ 11.72 (s, 1H), 11.72 (s, 1H), 10.38 (s, 1H), 8.54 (s, 1H), 8.39 (d, *J* = 7.9 Hz, 1H), 8.30 (d, *J* = 8.2 Hz, 1H), 7.92 (t, *J* = 8.1 Hz, 1H), 7.71 (t, *J* = 7.6 Hz, 1H), 7.65 (d, *J* = 8.9 Hz, 1H), 7.50 (t, *J* = 7.9 Hz, 2H), 7.40 (d, *J* = 8.8 Hz, 1H), 7.32 (t, *J* = 8.0 Hz, 3H). $^{13}$C NMR (101 MHz, DMSO-D6) δ 160.9, 152.5, 151.1, 134.3, 133.4, 129.9, 128.6, 128.1, 126.3, 125.9, 122.5, 118.1, 117.1. HRMS m/z: calcd. for $C_{20}H_{15}N_2O_3$ $[M+H]^+$ 331.1083, found 331.1082

**4.10.4.3** ***1-(6-oxo-5,6-dihydrophenanthridin-2-yl)-3-phenylurea*** **(10)** 69.4% yield (white solid); mp 367.6 - 367.9 ℃. $^{1}$H NMR (400 MHz, DMSO-D6) δ 11.66 (s, 1H), 8.78 (d, *J* = 1.9 Hz, 2H), 8.54 (s, 1H), 8.35 (t, *J* = 8.3 Hz, 2H), 7.90 (t, *J* = 7.6 Hz, 1H), 7.67 (t, *J* = 7.5 Hz, 1H), 7.53 (d, *J* = 9.9 Hz, 3H), 7.33 (dd, *J* = 16.8, 9.2 Hz, 3H), 7.00 (t, *J* = 7.3 Hz, 1H). $^{13}$C NMR (101 MHz, DMSO-D6) δ 160.8, 153.4, 140.2, 135.0,

134.5, 133.3, 132.3, 129.3, 128.3, 128.1, 126.3, 122.7, 122.3, 122.0, 118.7, 118.1, 117.1, 112.6. HRMS m/z: calcd. for $C_{20}H_{16}N_3O_2$ $[M+H]^+$ 330.1243, found 330.1253

**4.10.5 General synthetic procedure of compound 11~27**

Triethylamine (208 μL, 1.5 mmol) was added into a solution of 2-aminophenanthridin-6(5H)-one (0.30 g, 1 mmol), corresponding acid chloride compound (1mmol) and dichloromethane (5 mL). The reaction mixture was stirred for 8 h at room temperature. After the reaction, the mixture was filtered to remove solids, and the filtrate was removed under diminished pressure, and the residue was purified by chromatography on a silica gel column with 2:1 to 5:1 petroleum ether-ethyl acetate.

**4.10.5.1** ***N-(6-oxo-5,6-dihydrophenanthridin-2-yl)benzenesulfonamide*** **(11)**: 72.6% yield (pale pink solid); mp 281.5 - 282.3 □. $^1$H NMR (400 MHz, DMSO-D6) δ:11.66 (s, 1H), 10.29 (s, 1H), 8.32 (d, *J* = 7.7 Hz, 1H), 8.17 (d, *J* = 8.1 Hz, 1H), 7.98 (s, 1H), 7.89 (d, *J* = 4.1 Hz, 0H), 7.88 (s, 1H), 7.79 (d, *J* = 7.2 Hz, 2H), 7.65 (d, *J* = 7.5 Hz, 1H), 7.63 – 7.51 (m, 3H), 7.29 – 7.20 (m, 2H); $^{13}$C NMR (101 MHz, DMSO-D6) δ 160.8, 139.7, 134.2, 133.9, 133.4, 132.5, 129.7, 128.8, 128.1, 127.2, 126.3, 124.1, 122.5, 118.2, 117.4, 116.0; HRMS m/z: calcd. for $C_{19}H_{15}N_2O_3S$ $[M+H]^+$ 351.0803, found 351.0808;

**4.10.5.2** ***N-(6-oxo-5,6-dihydrophenanthridin-2-yl)-1-phenylmethanesulfonamide*** **(12)**: 82.1% yield (white solid ). mp 288.5 - 288.8 □. $^1$H NMR (400 MHz, DMSO-D6) δ: 11.74 (s, 1H), 9.91 (s, 1H), 8.38 (d, *J* = 7.2 Hz, 1H), 8.27 (d, *J* = 8.2 Hz, 1H), 8.08

(s, 1H), 7.95 (dd, *J* = 11.1, 4.0 Hz, 1H), 7.72 (t, *J* = 7.5 Hz, 1H), 7.45 – 7.29 (m, 7H), 4.55 (s, 2H); $^{13}$C NMR (101 MHz, DMSO-D6) δ: 161.0, 134.1, 133.7, 133.3, 131.5, 130.1, 129.0 – 128.5, 128.1, 126.3, 123.5, 122.8, 118.3, 117.5, 114.9. HRMS m/z: calcd. for $C_{20}H_{17}N_2O_3S$ $[M+H]^+$ 365.0960, found 365.0953;

**4.10.5.3** ***N-(6-oxo-5,6-dihydrophenanthridin-2-yl)propane-1-sulfonamide*** **(13)**: 80.8% yield (white solid ). mp 214.6 - 214.9 □. $^1$H NMR (500 MHz, DMSO-D6) δ 11.74 (s, 1H), 9.88 (s, 1H), 8.35 (d, *J* = 7.4 Hz, 1H), 8.29 (d, *J* = 8.0 Hz, 1H), 8.18 (s, 1H), 7.89 (s, 1H), 7.68 (t, *J* = 7.4 Hz, 1H), 7.42 (d, *J* = 10.4 Hz, 2H), 3.14 – 3.05 (m, 2H), 1.74 (dd, *J* = 15.0, 7.5 Hz, 2H), 0.96 (t, *J* = 7.4 Hz, 3H). $^{13}$C NMR (126 MHz, DMSO-D6) δ 161.0, 134.1, 134.0, 133.4, 133.34, 128.7, 128.1, 126.3, 123.8, 122.7, 118.4, 117.5, 115.4, 52.7, 17.2, 13.1. HRMS m/z: calcd. for $C_{16}H_{17}N_2O_3S$ $[M+H]^+$ 317.0960, found 317.0956;

**4.10.5.4** ***N-(6-oxo-5,6-dihydrophenanthridin-2-yl)propane-1-sulfonamide*** **(14)**: 78.5% yield (white solid ). mp 213.7 - 214.6 □. $^1$H NMR (500 MHz, DMSO-D6) δ 11.74 (s, 1H), 9.83 (s, 1H), 8.35 (d, *J* = 32.3 Hz, 2H), 8.17 (s, 1H), 7.93 (s, 1H), 7.71 (s, 1H), 7.41 (s, 2H), 3.13 (d, *J* = 1.1 Hz, 2H), 1.73 (d, *J* = 1.2 Hz, 2H), 1.39 (d, *J* = 5.7 Hz, 2H), 0.86 (s, 3H). $^{13}$C NMR (126 MHz, DMSO-D6) δ 161.0, 134.1, 134.1, 133.5, 133.3, 128.8, 128.7, 128.2, 126.38, 123.8, 123.8, 122.7, 118.4, 117.6, 115.4, 115.3, 50.7, 25.6, 21.2, 14.0. HRMS m/z: calcd. for $C_{17}H_{19}N_2O_3S$ $[M+H]^+$ 331.1116, found 331.1107;

**4.10.5.5** ***N-(6-oxo-5,6-dihydrophenanthridin-2-yl)cyclopentanesulfonamide*** **(15)**: 65.3% yield (white solid ). mp 226.3 - 226.9 ℃. $^1$H NMR (400 MHz, DMSO-D6) δ

11.71 (s, 1H), 9.76 (s, 1H), 8.34 (d, *J* = 7.9 Hz, 1H), 8.29 (d, *J* = 8.1 Hz, 1H), 8.12 (d, *J* = 1.9 Hz, 1H), 7.91 (t, *J* = 7.6 Hz, 1H), 7.68 (t, *J* = 7.5 Hz, 1H), 7.37 (dd, *J* = 12.9, 5.4 Hz, 2H), 1.96 – 1.85 (m, 4H), 1.71 – 1.61 (m, 2H), 1.58 – 1.48 (m, 2H), 1.28 – 1.15 (m, 3H). $^{13}$C NMR (101 MHz, DMSO-D6) δ 160.9, 134.0, 133.9, 133.5, 133.4, 128.8, 128.1, 126.2, 124.0, 122.7, 118.4, 117.5, 115.4, 60.1, 27.9, 25.9. HRMS m/z: calcd. for $C_{18}H_{19}N_2O_3S$ $[M+H]^+$ 343.1116, found 343.1112

**4.10.5.6** ***N-(6-oxo-5,6-dihydrophenanthridin-2-yl)cyclohexanesulfonamide*** **(16)**: 79.2% yield (white solid ). mp 230.2 - 230.9 □. $^1$H NMR (500 MHz, DMSO-D6) δ 11.75 (s, 1H), 9.82 (s, 1H), 8.35 (d, *J* = 7.7 Hz, 1H), 8.27 (d, *J* = 8.1 Hz, 1H), 8.16 (s, 1H), 7.91 (t, *J* = 7.3 Hz, 1H), 7.68 (t, *J* = 7.4 Hz, 1H), 7.42 (d, *J* = 8.7 Hz, 1H), 7.37 (d, *J* = 8.7 Hz, 1H), 3.02 (t, *J* = 10.1 Hz, 1H), 2.08 (d, *J* = 12.0 Hz, 2H), 1.76 (s, 2H), 1.64 – 1.53 (m, 2H), 1.44 (d, *J* = 10.2 Hz, 2H), 1.21 (d, *J* = 12.3 Hz, 2H). $^{13}$C NMR (126 MHz, DMSO-D6) δ 161.0, 134.1, 133.8, 133.6, 133.3, 128.7, 128.1, 126.4, 123.3, 122.7, 118.36, 117.5, 114.7, 59.4, 58.8, 27.8, 26.5, 25.8, 25.5, 25.2, 24.8. HRMS m/z: calcd for $C_{19}H_{21}N_2O_3S$ $[M+H]^+$ 357.1273, found 357.1264 ;

**4.10.5.7** ***2-chloro-N-(6-oxo-5,6-dihydrophenanthridin-2-yl)benzenesulfonamide*** **(17):** 79.8% yield(white solid); mp 275.4 - 275.8 □. $^1$H NMR (500 MHz, DMSO-D6) δ 11.72 (s, 1H), 10.72 (s, 1H), 8.32 (d, *J* = 7.9 Hz, 1H), 8.16 (d, *J* = 8.1 Hz, 1H), 8.10 (dd, *J* = 7.9, 1.4 Hz, 1H), 8.04 (d, *J* = 1.9 Hz, 1H), 7.90 (dd, *J* = 11.2, 4.1 Hz, 1H), 7.70 – 7.64 (m, 2H), 7.63 – 7.58 (m, 1H), 7.51 (dd, *J* = 11.8, 4.5 Hz, 1H), 7.29 (dd, *J* = 9.4, 7.3 Hz, 2H). $^{13}$C NMR (126 MHz, DMSO-D6) δ 160.8, 136.9, 135.1, 134.0, 133.8, 133.51, 132.3, 132.1, 131.9, 131.3, 128.8, 128.2, 126.31, 123.3, 122.4, 118.2,

117.5, 114.9. HRMS m/z: calcd. for $C_{19}H_{14}ClN_2O_3S$ $[M+H]^+$ 385.0414, found 385.0406;

**4.10.5.8** ***6-methoxy-N-(6-oxo-5,6-dihydrophenanthridin-2-yl)benzenesulfonamide*** **(18)**: 81.3% yield (white solid). mp 298.4 - 299.3 □. $^1$H NMR (400 MHz, DMSO-D6) δ: 11.61 (s, 1H), 9.98 (s, 1H), 8.34 – 8.27 (m, 1H), 8.15 (d, J = 8.1 Hz, 1H), 7.98 (d, J = 1.5 Hz, 1H), 7.92 – 7.85 (m, 1H), 7.77 (dd, J = 7.8, 1.6 Hz, 1H), 7.65 (t, *J* = 7.5 Hz, 1H), 7.56 – 7.50 (m, 1H), 7.22 (dd, *J* = 9.8, 5.3 Hz, 2H), 7.17 (d, *J* = 8.3 Hz, 1H), 7.00 (t, *J* = 7.6 Hz, 1H), 3.95 (s, 3H); $^{13}$C NMR (101 MHz, DMSO-D6) δ: 160.9, 156.8, 135.6, 133.9, 133.5, 132.8, 130.8, 128.7, 128.2, 126.6, 126.3, 123.5, 122.3, 120.6, 118.0, 117.2, 115.0, 113.2, 56.6. HRMS m/z: calcd. for $C_{20}H_{17}N_2O_4S$ $[M+H]^+$ 381.0909, found 381.0905;

**4.10.5.9** ***2-(tert-butyl)-N-(6-oxo-5,6-dihydrophenanthridin-2-yl)benzenesulfonamide*** **(19)**: 81.8% yield (white solid); mp 267.4 - 267.7 □. $^1$H NMR (500 MHz, DMSO-D6) δ 11.67 (s, 1H), 10.28 (s, 1H), 8.33 (s, 1H), 8.11 (s, 1H), 7.96 (s, 1H), 7.86 (s, 1H), 7.70 (d, *J* = 42.4 Hz, 3H), 7.56 (s, 2H), 7.28 (s, 2H), 1.22 (s, 9H). $^{13}$C NMR (126 MHz, DMSO-D6) δ 161.0, 156.4, 137.2, 134.1, 134.0, 133.5, 132.7, 128.8, 128.2, 128.2, 127.2, 126.6, 126.3, 124.0, 124.0, 122.4, 122.4, 118.2, 117.3, 117.4, 115.7, 115.6, 35.6, 31.9. HRMS m/z: calcd. for $C_{23}H_{23}N_2O_3S$ $[M+H]^+$ 407.1429, found 407.1426 ;

**4.10.5.10** ***2-chloro-N-(6-oxo-5,6-dihydrophenanthridin-2-yl)benzenesulfonamide*** **(20)**: 80.2% yield(white solid); mp 268.4 - 268.9 □. $^1$H NMR (500 MHz, DMSO-D6) δ: 11.71 (s, 1H), 10.39 (s, 1H), 8.34 (d, *J* = 7.9 Hz, 1H), 8.21 (d, *J* = 8.2 Hz, 1H), 8.03

(s, 0H), 8.01 (d, *J* = 2.1 Hz, 1H), 7.93 – 7.84 (m, 1H), 7.81 – 7.73 (m, 2H), 7.71 – 7.65 (m, 1H), 7.66 – 7.60 (m, 2H), 7.28 (d, *J* = 8.7 Hz, 1H), 7.21 (dd, *J* = 8.7, 2.2 Hz, 1H). $^{13}$C NMR (126 MHz, DMSO-D6) δ: 160.9, 138.2 – 138.1, 134.5, 133.9, 133.5, 132.1, 129.9, 129.2, 128.8, 128.1, 126.3, 124.4, 122.5, 118.3, 117.5, 116.4. HRMS m/z: calcd. for $C_{19}H_{14}ClN_2O_3S$ $[M+H]^+$ 385.0414, found 385.0398;

**4.10.5.11** ***2-methoxy-N-(6-oxo-5,6-dihydrophenanthridin-2-yl)benzenesulfonamide*** **(21)**: 91.0% yield (white solid); mp 285.8 - 286.7 □. $^1$H NMR (500 MHz, DMSO-D6) δ: 11.64 (s, 1H), 10.14 (s, 1H), 8.30 (d, *J* = 8.7 Hz, 1H), 8.15 (d, *J* = 8.1 Hz, 1H), 7.97 (d, *J* = 1.8 Hz, 1H), 7.85 (t, *J* = 7.6 Hz, 1H), 7.70 (d, *J* = 8.9 Hz, 2H), 7.63 (t, *J* = 7.5 Hz, 1H), 7.21 (dt, *J* = 8.7, 5.4 Hz, 2H), 7.02 (d, *J* = 8.9 Hz, 2H), 3.74 (s, 3H). $^{13}$C NMR (126 MHz, DMSO-D6) δ: 162.9, 160.9, 134.0, 133.5, 132.8, 131.4, 129.5, 128.7, 128.1, 126.3, 123.9, 122.5, 118.1, 117.4, 115.6, 114.8, 56.0. HRMS m/z: calcd. for $C_{20}H_{17}N_2O_4S$ $[M+H]^+$ 381.0909, found 381.0892 ;

**4.10.5.12** ***2-cyano-N-(6-oxo-5,6-dihydrophenanthridin-2-yl)benzenesulfonamide*** **(22)**: 79.2% yield(white solid). mp 290.6 - 291.3 □. $^1$H NMR (500 MHz, DMSO-D6) δ 11.78 (d, *J* = 34.8 Hz, 1H), 10.54 (d, *J* = 34.4 Hz, 1H), 8.45 (s, 1H), 8.42 – 8.30 (m, 2H), 8.27 (t, *J* = 8.6 Hz, 1H), 8.20 – 8.11 (m, 2H), 8.09 (d, *J* = 7.5 Hz, 1H), 8.01 (d, *J* = 6.1 Hz, 1H), 7.92 (dd, *J* = 19.4, 11.5 Hz, 1H), 7.86 – 7.76 (m, 1H), 7.77 – 7.66 (m, 1H), 7.44 – 7.22 (m, 2H). $^{13}$C NMR (126 MHz, DMSO-D6) δ 161.0, 161.0, 141.1, 141.0, 137.1, 137.0, 134.7, 134.7, 133.6, 133.5, 131.8, 131.7, 131.3, 131.3, 130.8, 130.8, 128.9, 128.8, 128.2, 128.1, 126.4, 126.3, 124.7, 124.6, 122.7, 122.6, 118.4,

118.4, 117.9, 117.9, 117.6, 117.6, 117.0, 116.9, 113.0, 113.0. HRMS m/z: calcd. for $C_{20}H_{14}N_3O_3S$ $[M+H]^+$ 376.0756, found 376.0756;

**4.10.5.13** ***3-cyano-N-(6-oxo-5,6-dihydrophenanthridin-2-yl)benzenesulfonamide*** **(23)** 82.3% yield (white solid). mp 282.7 - 283.2 □. $^1$H NMR (400 MHz, DMSO-D6) δ 11.72 (s, 1H), 10.44 (s, 1H), 8.34 (d, *J* = 7.8 Hz, 1H), 8.22 (d, *J* = 8.1 Hz, 1H), 8.02 (d, *J* = 1.8 Hz, 1H), 7.89 (t, *J* = 7.6 Hz, 1H), 7.82 (s, 1H), 7.75 – 7.66 (m, 3H), 7.59 (t, *J* = 7.9 Hz, 1H), 7.30 (d, *J* = 8.7 Hz, 1H), 7.25 – 7.20 (m, 1H). $^{13}$C NMR (101 MHz, DMSO-D6) δ 161.0, 141.6, 134.5, 134.3, 133.9, 133.5, 133.4, 132.0, 131.8, 128.8, 128.1, 126.8, 126.3, 126.0, 124.4, 122.5, 118.3, 117.5, 116.5. HRMS m/z: calcd. for $C_{19}H_{14}ClN_2O_3S$ $[M+H]^+$ 385.0414, found 385.0421

**4.10.5.14** ***5-chloro-2-methoxy-N-(6-oxo-5,6-dihydrophenanthridin-2-yl)benzenes ulfonamide*** **(24)** :72.6% yield (white solid). mp 298.4 - 298.8 □. $^1$H NMR (400 MHz, DMSO-D6) δ: 11.65 (s, 1H), 10.17 (s, 0H), 10.17 (s, 1H), 8.32 (d, *J* = 7.9 Hz, 1H), 8.18 (d, *J* = 8.2 Hz, 1H), 7.99 (s, 1H), 7.87 (s, 1H), 7.71 (s, 1H), 7.70 (s, 0H), 7.66 (t, *J* = 7.5 Hz, 1H), 7.61 (dd, *J* = 8.9, 2.6 Hz, 1H), 7.23 (d, *J* = 9.6 Hz, 3H), 3.96 (s, 3H); $^{13}$C NMR (101 MHz, DMSO-D6) δ: 160.9, 155.8, 135.1, 134.2, 133.9, 133.6, 132.2, 129.8, 128.8, 128.2, 126.3, 124.2 123.8, 122.3, 118.1, 117.4, 115.5, 57.1. HRMS m/z: calcd. for $C_{20}H_{16}N_2O_4S$ $[M+H]^+$ 415.0519, found 415.0522;

**4.10.5.15** ***N-(6-oxo-5,6-dihydrophenanthridin-2-yl)thiophene-2-sulfonamide*** **(25):** 75.5% (white solid). mp 296.8 - 297.1 □. $^1$H NMR (500 MHz, DMSO-D6) δ: 11.81 – 11.69 (m, 1H), 10.51 (dd, *J* = 21.1, 9.9 Hz, 1H), 8.34 (d, *J* = 7.4 Hz, 1H), 8.20 (d, *J* = 7.7 Hz, 1H), 8.13 – 8.01 (m, 1H), 7.90 (d, *J* = 6.8 Hz, 2H), 7.76 – 7.65 (m, 1H), 7.60

(d, *J* = 17.4 Hz, 1H), 7.31 (dt, *J* = 21.7, 10.7 Hz, 2H), 7.21 – 7.07 (m, 1H). $^{13}$C NMR (126 MHz, DMSO-D6) δ: 161.0, 140.2, 134.5, 134.3, 133.6, 133.5, 133.0, 132.3, 128.1, 126.3, 124.4, 122.5, 117.4, 116.3. HRMS m/z: calcd. for $C_{17}H_{13}N_2O_3S_2$ $[M+H]^+$ 357.0368, found 357.0366;

**4.10.5.16** ***N-(6-oxo-5,6-dihydrophenanthridin-2-yl)naphthalene-2-sulfonamide*** **(26)**: 85.9% (white solid). mp 291.4 - 292.3 □. $^1$H NMR (500 MHz, DMSO-D6) δ 11.68 (s, 1H), 10.55 (s, 1H), 8.51 (s, 1H), 8.31 (d, *J* = 7.3 Hz, 1H), 8.19 (d, *J* = 7.6 Hz, 1H), 8.12 (t, *J* = 8.5 Hz, 2H), 8.08 (s, 1H), 8.00 (d, *J* = 7.5 Hz, 1H), 7.87 (t, *J* = 8.4 Hz, 2H), 7.66 (d, *J* = 7.8 Hz, 2H), 7.64 – 7.60 (m, 1H), 7.26 (d, *J* = 6.5 Hz, 2H). $^{13}$C NMR (126 MHz, DMSO-D6) δ 160.9, 136.9, 134.7, 134.2, 133.9, 133.4, 132.5, 132.0, 129.9, 129.7, 129.5, 128.7, 128.6, 128.3, 128.1, 126.3, 124.0, 122.7, 122.5, 118.2, 117.4, 115.9. HRMS m/z: calcd. for $C_{23}H_{17}N_2O_3S$ $[M+H]^+$ 401.0960, found 401.0968;

**4.10.5.17**

***N-(6-oxo-5,6-dihydrophenanthridin-2-yl)-2,3-dihydrobenzofuran-5-sulfonamide*** **(27)**: 83.6% (white solid). mp 280.4 - 280.9 □. $^1$H NMR (500 MHz, DMSO-D6) δ 11.65 (s, 1H), 10.15 (s, 1H), 8.31 (d, *J* = 7.1 Hz, 1H), 8.17 (d, *J* = 6.8 Hz, 1H), 7.99 (s, 1H), 7.87 (s, 1H), 7.65 (s, 2H), 7.55 (d, *J* = 7.9 Hz, 1H), 7.35 – 7.17 (m, 2H), 6.84 (d, *J* = 6.7 Hz, 1H), 4.67 – 4.46 (m, 2H), 3.18 (d, *J* = 7.2 Hz, 2H). $^{13}$C NMR (126 MHz, DMSO-D6) δ 163.7, 160.9, 134.0, 133.5, 132.9, 131.5, 129.2, 128.7, 128.2, 126.3, 124.6, 123.8, 122.4, 118.2, 117.3, 115.5, 109.8, 72.6, 28.2. HRMS m/z: calcd. for $C_{21}H_{17}N_2O_4S$ $[M+H]^+$ 393.0909, found 393.0899;

**Supporting Information**

Supporting information related to this article can be found at http://dx.doi.org/

**Author Contributions**

Zhimin Zhang designed the study. Yanle Zhi, Shu Wang, Wenhai Huang and Shenxin Zeng prepared all simples for analysis. Zhimin Zhang, Yanle Zhi, Meihao Liang, Chixiao Zhang, Zhen Ma and Zunyuan Wang collected and analysed the data. Zhimin Zhang and Zhengrong Shen interpreted the results and wrote the manuscript. All authors gave final approval for publication.

**Conflict of Interest**

The authors declare no competing financial interest.

**Acknowledgments**

This work was financially supported by The National Natural Science Funds of China (81803372), Key Laboratory of Neuropsychiatric Drug Research of Zhejiang Province (2019E10021), Doctoral Fund of Zhejiang Academy of Medical Sciences (A11701Q) and Health Commission of Zhejiang Province (2019RC141).

**Abbreviations**

BET Bromodomain and extra-terminal

BRD4 Bromodomain-containing protein 4

P-TEFb positive transcription elongation factor b

KAc acetylated lysine

WPF Trp81, Pro82, and Phe83

SAR structure−activity relationship

HLMs human liver microsomes

## References

[1] P. Filippakopoulos, S. Knapp, Targeting bromodomains: epigenetic readers of lysine acetylation, Nat. Rev. Drug. Discov. 13 (2014) 339-358.

[2] U. Schaefer, Pharmacological Inhibition of Bromodomain-Containing Proteins in Inflammation, Csh. Perspect. Biol. 6 (2014).

[3] C. Banerjee, N. Archin, D. Michaels, A.C. Belkina, G.V. Denis, J. Bradner, P. Sebastiani, D.M. Margolis, M. Montano, BET bromodomain inhibition as a novel strategy for reactivation of HIV-1, J. Leukocyte Biol. 92 (2012) 1147-1154.

[4] D. Boehm, R.J. Conrad, M. Ott, Bromodomain Proteins in HIV Infection, Viruses-Basel, 5 (2013) 1571-1586.

[5] K. Fujinaga, Z.P. Luo, F. Schaufele, B.M. Peterlin, Visualization of Positive Transcription Elongation Factor b (P-TEFb) Activation in Living Cells, J. Biol. Chem. 290 (2015) 1829-1836.

[6] M.C. Patel, M. Debrosse, M. Smith, A. Dey, W. Huynh, N. Sarai, T.D. Heightman, T. Tamura, K. Ozato, BRD4 Coordinates Recruitment of Pause Release Factor P-TEFb and the Pausing Complex NELF/DSIF To Regulate Transcription Elongation of Interferon-Stimulated Genes, Mol. Cell. Biol. 33 (2013) 2497-2507.

[7] Q. Xiang, C. Wang, Y. Zhang, X. Xue, M. Song, C. Zhang, C. Li, C. Wu, K. Li, X. Hui, Y. Zhou, J.B. Smaill, A.V. Patterson, D. Wu, K. Ding, Y. Xu, Discovery and optimization of 1-(1H-indol-1-yl)ethanone derivatives as CBP/EP300 bromodomain inhibitors for the treatment of castration-resistant prostate cancer, Eur. J. Med. Chem. 147 (2018) 238-252.

[8] P. Filippakopoulos, S. Picaud, M. Mangos, T. Keates, J.P. Lambert, D. Barsyte-Lovejoy, I. Felletar, R. Volkmer, S. Muller, T. Pawson, A.C. Gingras, C.H. Arrowsmith, S. Knapp, Histone Recognition and Large-Scale Structural Analysis of the Human Bromodomain Family, Cell, 149 (2012) 214-231.

[9] L.L. Fu, M. Tian, X. Li, J.J. Li, J. Huang, L. Ouyang, Y.H. Zhang, B. Liu, Inhibition of BET bromodomains as a therapeutic strategy for cancer drug discovery, Oncotarget, 6 (2015) 5501-5516.

[10] S.G. Smith, M.M. Zhou, The Bromodomain: A New Target in Emerging Epigenetic Medicine,

Acs Chem. Biol. 11 (2016) 598-608.

[11] I. Casciuc, D. Horvath, A. Gryniukova, K.A. Tolmachova, O.V. Vasylchenko, P. Borysko, Y.S. Moroz, J. Bajorath, A. Varnek, Pros and cons of virtual screening based on public "Big Data": In silico mining for new bromodomain inhibitors, Eur. J. Med. Chem. 165 (2019) 258-272.

[12] J. Hu, Y. Wang, Y. Li, D. Cao, L. Xu, S. Song, M.S. Damaneh, J. Li, Y. Chen, X. Wang, L. Chen, J. Shen, Z. Miao, B. Xiong, Structure-based optimization of a series of selective BET inhibitors containing aniline or indoline groups, Eur. J. Med. Chem. 150 (2018) 156-175.

[13] J. Li, P. Wang, B. Zhou, J. Shi, J. Liu, X. Li, L. Fan, Y. Zheng, L. Ouyang, Development of 4,5-dihydro-benzodiazepinone derivatives as a new chemical series of BRD4 inhibitors, Eur. J. Med. Chem. 121 (2016) 294-299.

[14] X. Xue, Y. Zhang, C. Wang, M. Zhang, Q. Xiang, J. Wang, A. Wang, C. Li, C. Zhang, L. Zou, R. Wang, S. Wu, Y. Lu, H. Chen, K. Ding, G. Li, Y. Xu, Benzoxazinone-containing 3,5-dimethylisoxazole derivatives as BET bromodomain inhibitors for treatment of castration-resistant prostate cancer, Eur. J. Med. Chem. 152 (2018) 542-559.

[15] L. Wang, J.K. Pratt, T. Soltwedel, G.S. Sheppard, S.D. Fidanze, D. Liu, L.A. Hasvold, R.A. Mantei, J.H. Holms, W.J. McClellan, M.D. Wendt, C. Wada, R. Frey, T.M. Hansen, R. Hubbard, C.H. Park, L. Li, T.J. Magoc, D.H. Albert, X. Lin, S.E. Warder, P. Kovar, X. Huang, D. Wilcox, R. Wang, G. Rajaraman, A.M. Petros, C.W. Hutchins, S.C. Panchal, C. Sun, S.W. Elmore, Y. Shen, W.M. Kati, K.F. McDaniel, Fragment-Based, Structure-Enabled Discovery of Novel Pyridones and Pyridone Macrocycles as Potent Bromodomain and Extra-Terminal Domain (BET) Family Bromodomain Inhibitors, J. Med. Chem. 60 (2017) 3828-3850.

[16] Y. Zhao, B. Zhou, L. Bai, L. Liu, C.Y. Yang, J.L. Meagher, J.A. Stuckey, D. McEachern, S. Przybranowski, M. Wang, X. Ran, A. Aguilar, Y. Hu, J.W. Kampf, X. Li, T. Zhao, S. Li, B. Wen, D. Sun, S. Wang, Structure-Based Discovery of CF53 as a Potent and Orally Bioavailable Bromodomain and Extra-Terminal (BET) Bromodomain Inhibitor, J. Med. Chem. 61 (2018) 6110-6120.

[17] A. Alqahtani, K. Choucair, M. Ashraf, D.M. Hammouda, A. Alloghbi, T. Khan, N. Senzer, J. Nemunaitis, Bromodomain and extra-terminal motif inhibitors: a review of preclinical and clinical advances in cancer therapy, Futur. Sci. Oa. 5 (2019).

[18] N.H. Theodoulou, N.C.O. Tomkinson, R.K. Prinjha, P.G. Humphreys, Clinical progress and

pharmacology of small molecule bromodomain inhibitors, Curr. Opin. Chem. Biol. 33 (2016) 58-66.

[19] P. Filippakopoulos, J. Qi, S. Picaud, Y. Shen, W.B. Smith, O. Fedorov, E.M. Morse, T. Keates, T.T. Hickman, I. Felletar, M. Philpott, S. Munro, M.R. McKeown, Y.C. Wang, A.L. Christie, N. West, M.J. Cameron, B. Schwartz, T.D. Heightman, N. La Thangue, C.A. French, O. Wiest, A.L. Kung, S. Knapp, J.E. Bradner, Selective inhibition of BET bromodomains, Nature, 468 (2010) 1067-1073.

[20] M.A. Dawson, R.K. Prinjha, A. Dittmann, G. Giotopoulos, M. Bantscheff, W.I. Chan, S.C. Robson, C.W. Chung, C. Hopf, M.M. Savitski, C. Huthmacher, E. Gudgin, D. Lugo, S. Beinke, T.D. Chapman, E.J. Roberts, P.E. Soden, K.R. Auger, O. Mirguet, K. Doehner, R. Delwel, A.K. Burnett, P. Jeffrey, G. Drewes, K. Lee, B.J.P. Huntly, T. Kouzarides, Inhibition of BET recruitment to chromatin as an effective treatment for MLL-fusion leukaemia, Nature, 478 (2011) 529-533.

[21] Y.L. Khmelnitsky, V.V. Mozhaev, I.C. Cotterill, P.C. Michels, S. Boudjabi, V. Khlebnikov, M.M. Reddy, G.S. Wagner, H.C. Hansen, In vitro biosynthesis, isolation, and identification of predominant metabolites of 2-(4-(2-hydroxyethoxy)-3,5-dimethylphenyl)-5,7-dimethoxyquinazolin-4(3H)-one (RVX-208), Eur. J. Med. Chem. 64 (2013) 121-128.

[22] S. Picaud, C. Wells, I. Felletar, D. Brotherton, S. Martin, P. Savitsky, B. Diez-Dacal, M. Philpott, C. Bountra, H. Lingard, O. Fedorov, S. Muller, P.E. Brennan, S. Knapp, P. Filippakopoulos, RVX-208, an inhibitor of BET transcriptional regulators with selectivity for the second bromodomain, P. Natl. Acad. Sci. USA, 110 (2013) 19754-19759.

[23] Z. Zhang, L. Gu, B. Wang, W. Huang, Y. Zhang, Z. Ma, S. Zeng, Z. Shen, Discovery of novel coumarin derivatives as potent and orally bioavailable BRD4 inhibitors based on scaffold hopping, J. Enzyme Inhib. Med. Chem. 34 (2019) 808-817.

[24] Y. Feng, S. Xiao, Y. Chen, H. Jiang, N. Liu, C. Luo, S. Chen, H. Chen, Design, synthesis and biological evaluation of benzo[cd]indol-2(1H)-ones derivatives as BRD4 inhibitors, Eur. J. Med. Chem. 152 (2018) 264-273.

[25] J. Hu, Y. Wang, Y. Li, L. Xu, D. Cao, S. Song, M.S. Damaneh, X. Wang, T. Meng, Y.L. Chen, J. Shen, Z. Miao, B. Xiong, Discovery of a series of dihydroquinoxalin-2(1H)-ones as selective BET inhibitors from a dual PLK1-BRD4 inhibitor, Eur. J. Med. Chem. 137 (2017)

176-195.

[26] Z. Liu, B. Tian, H. Chen, P. Wang, A.R. Brasier, J. Zhou, Discovery of potent and selective BRD4 inhibitors capable of blocking TLR3-induced acute airway inflammation, Eur. J. Med. Chem. 151 (2018) 450-461.

[27] K.F. McDaniel, L. Wang, T. Soltwedel, S.D. Fidanze, L.A. Hasvold, D. Liu, R.A. Mantei, J.K. Pratt, G.S. Sheppard, M.H. Bui, E.J. Faivre, X. Huang, L. Li, X. Lin, R. Wang, S.E. Warder, D. Wilcox, D.H. Albert, T.J. Magoc, G. Rajaraman, C.H. Park, C.W. Hutchins, J.J. Shen, R.P. Edalji, C.C. Sun, R. Martin, W. Gao, S. Wong, G. Fang, S.W. Elmore, Y. Shen, W.M. Kati, Discovery of N-(4-(2,4-Difluorophenoxy)-3-(6-methyl-7-oxo-6,7-dihydro-1H-pyrrolo [2,3-c]pyridin -4-yl)phenyl)ethanesulfonamide (ABBV-075/Mivebresib), a Potent and Orally Available Bromodomain and Extraterminal Domain (BET) Family Bromodomain Inhibitor, J. Med. Chem. 60 (2017) 8369-8384.

[28] T. Halgren, New method for fast and accurate binding-site identification and analysis, Chem. Biol. & Drug Des. 69 (2007) 146-148.

[29] T.A. Halgren, Identifying and Characterizing Binding Sites and Assessing Druggability, J. Chem. Inf. Model. 49 (2009) 377-389.

[30] J.A. Mertz, A.R. Conery, B.M. Bryant, P. Sandy, S. Balasubramanian, D.A. Mele, L. Bergeron, R.J. Sims, 3rd, Targeting MYC dependence in cancer by inhibiting BET bromodomains, P. Natl. Acad. Sci. USA, 108 (2011) 16669-16674.

[31] J.E. Delmore, G.C. Issa, M.E. Lemieux, P.B. Rahl, J.W. Shi, H.M. Jacobs, E. Kastritis, T. Gilpatrick, R.M. Paranal, J. Qi, M. Chesi, A.C. Schinzel, M.R. McKeown, T.P. Heffernan, C.R. Vakoc, P.L. Bergsagel, I.M. Ghobrial, P.G. Richardson, R.A. Young, W.C. Hahn, K.C. Anderson, A.L. Kung, J.E. Bradner, C.S. Mitsiades, BET Bromodomain Inhibition as a Therapeutic Strategy to Target c-Myc, Cell, 146 (2011) 903-916.

## Highlights

Novel phenanthridin-6(5*H*)-one derivatives have been synthesized as high selective BET inhibitors.

Compound **24** significantly inhibited the growth of A549 cells with $IC_{50}$ value of 0.75 μM.

C-myc may be involved in compound **24** induced the arrest of G1/M phase and apoptosis on A549 cells.

Compound **24** exhibited satisfying PK profiles with a $T_{1/2}$ of 3.87 h and F% of 36.6%.